Electronic Supplementary Material (ESI) for Soft Matter.

Unusual Polysaccharide Rheology of Aqueous Dispersions of Soft Phytoglycogen Nanoparticles

Hurmiz Shamana,[1] Michael Grossutti,[1] Erzsebet Papp-Szabo,[1] Carley Miki,[1,2] and John R. Dutcher[*,1]*

[1]Department of Physics, University of Guelph, Guelph, ON N1G 2W1

[2]Mirexus Biotechnologies Inc., Guelph, ON N1G 3M5

Supplementary Information

This document contains additional technical details and 9 supporting data figures.

* correspondence to: dutcher@uoguelph.ca

Evaluation of Homogenization Time, Pre-Shear Rate and Equilibration Time for Aqueous Phytoglycogen Dispersions

To ensure proper mixing of the aqueous phytoglycogen dispersions and the reproducibility of the rheology experiments, we investigated the effect of varying the homogenization time, pre-shear rate and equilibration time.

In Figure S1, we show the relative zero-shear viscosity $\eta_r = \eta_0/\eta_s$, where η_0 is the zero-shear viscosity of the sample and η_s is the viscosity of the water solvent, as a function of the total homogenization time for aqueous phytoglycogen dispersions of concentrations C = 20% w/w and C = 27.5% w/w. In Figure S1, each data point corresponds to a different dispersion. For the C = 20% w/w dispersions, the relative viscosity η_r reaches a plateau after only about 1 min of homogenization. For the C = 27.5% w/w dispersions, a much longer homogenization time of 20 min was required to reach a plateau in the relative viscosity η_r values. The presence of a plateau in the relative viscosity η_r versus homogenization time data was used as an indication that the dispersions were well mixed. Based on this result, we decided to homogenize dispersions with concentrations $C \leq$ 20% w/w for 3 min, since this is sufficient to properly mix a C = 20% w/w dispersion, and therefore it should be sufficient to homogenize dispersions with smaller concentrations. Dispersions with concentrations 20 < $C \leq$ 27.5% w/w were homogenized in 3 min intervals separated by 1 min rest periods for an overall homogenization time of 21 min. Since this value of the homogenization time lies within the plateau region of Figure S1b, corresponding to a C = 27.5% w/w dispersion, it should be sufficient to homogenize dispersions with concentrations 20 < $C \leq$ 27.5% w/w. For slightly larger concentrations (C = 29.07, 30.05 and 32.01% w/w), we chose a longer homogenization time of 40 min.

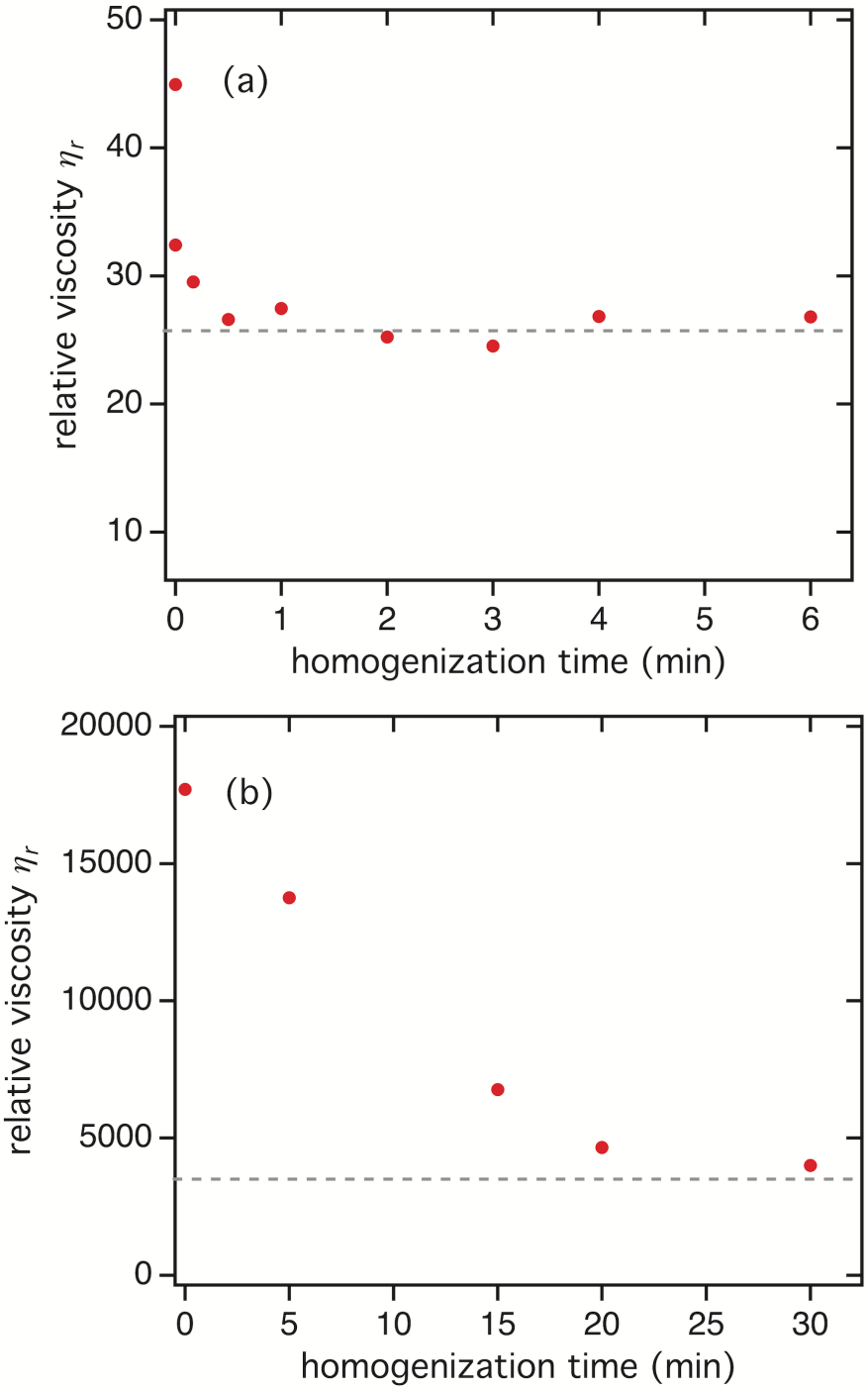

Figure S1: Relative viscosity η_r vs. homogenization time for aqueous phytoglycogen dispersions with concentrations (a) C = 20% w/w and (b) C = 27.5% w/w. The dashed horizontal lines are guides to the eye indicating the asymptotic value of η_r.

We also varied the pre-shear rate $\dot{\gamma}_{\mathrm{pre-shear}}$ and the equilibration time t_{equil} prior to measuring the zero-shear viscosity. We used pre-shear rates of $\dot{\gamma}_{\mathrm{pre-shear}}$ = 0 s^{-1}, 10 s^{-1} and 100 s^{-1}, which were applied to the sample for 10 min. For each of these pre-shear rates, the sample was allowed to equilibrate for different equilibration times t_{equil} that varied between 0 and 60 min. Immediately after the equilibration time, the dependence of η_r on $\dot{\gamma}$ was measured, and the results are shown in Figure S2. Each pre-shear procedure was initiated immediately following the previous rheology measurement, with the procedure repeated on the same sample until the 15 $\eta_r(\dot{\gamma})$ curves shown in Figure S2 were collected. All of the $\eta_r(\dot{\gamma})$ curves are in reasonable agreement, indicating that the measured viscosity values do not vary significantly with changes to the pre-shear procedure and suggesting the lack of significant aging effects. This insensitivity to the pre-shear conditions can be also be seen by comparing the very good agreement obtained for the zero-shear viscosity η_0 values calculated for each curve using Equation 1, as shown in Figure S3. The arrows in Figure S3 indicate the order in which the data points were obtained, with the $\dot{\gamma}_{\mathrm{pre-shear}}$ = 0 s^{-1} data set (red symbols) measured first, followed by the $\dot{\gamma}_{\mathrm{pre-shear}}$ = 10 s^{-1} data set (blue symbols), and then followed by the $\dot{\gamma}_{\mathrm{pre-shear}}$ = 100 s^{-1} data set (green symbols). Each data set was collected over a time period of about 2.5 h for a total measurement time of approximately 8 h. Because these measurements were performed on the same sample, it is possible that a small amount of solvent evaporation occurred through the solvent trap and the bead of oil over the course of the 8 h measurement, which is the most likely source of the discrepancy between the curves in Figure S3. Nevertheless, there is good agreement between the data sets in Figure S3, which suggests that the zero-shear viscosity η_0 is insensitive to the pre-shear conditions.

Because of the insensitivity to the pre-shear conditions, we chose a convenient pre-shear rate of $\dot{\gamma}_{\mathrm{pre-shear}}$ = 100 s^{-1} for 10 min (corresponding to the green symbols in Figure S3) and an equilibration time t_{equil} = 10 min. This pre-shear procedure was performed before every rheology measurement.

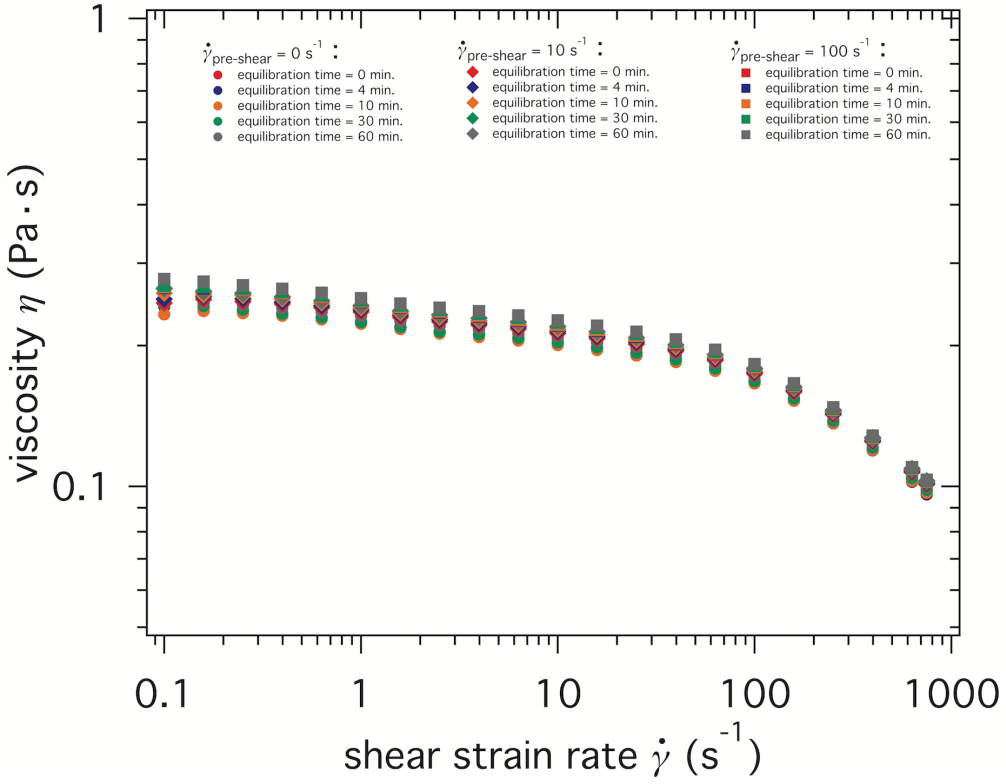

Figure S2: Viscosity η versus shear strain rate $\dot{\gamma}$ for an aqueous phytoglycogen dispersion of concentration C = 23.98 % w/w. Pre-shear rates of $\dot{\gamma}_{\mathrm{pre-shear}}$ = 0 s^{-1}, 10 s^{-1}, and 100 s^{-1} were applied for 10 min followed by an equilibration period t_{equil} ranging between 0 – 60 min. The 15 curves were collected during a time period of approximately 8 h.

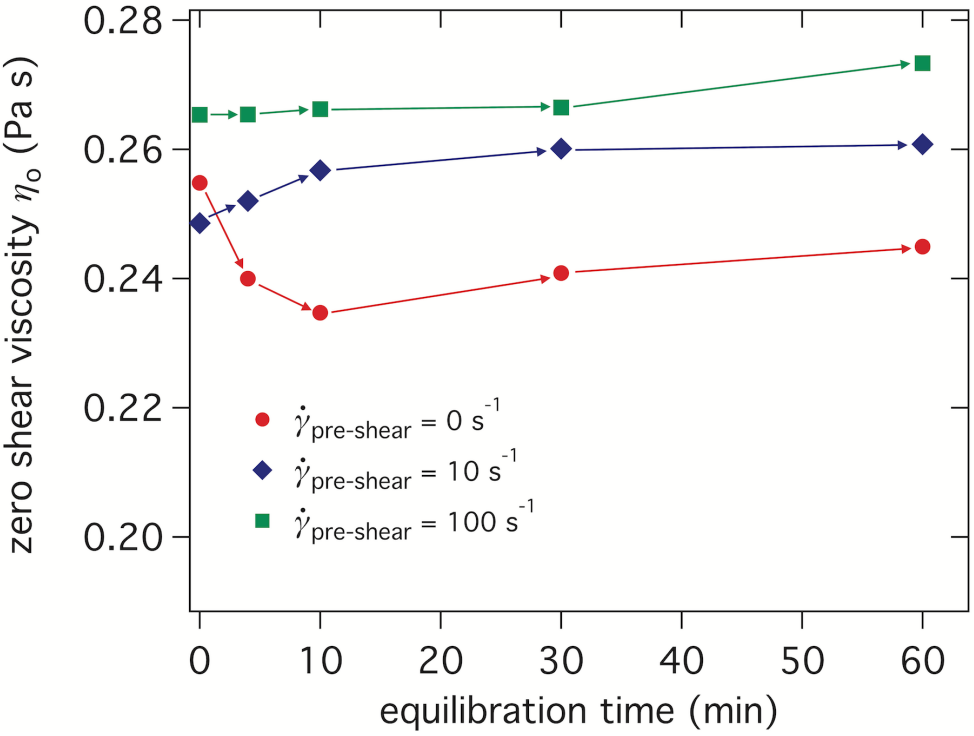

Figure S3: Zero shear viscosity η_0 vs. equilibration time t_{equil} for pre-shear rates of $\dot{\gamma}_{pre-shear}$ = 0 s^{-1} (red circles), 10 s^{-1} (blue diamonds), and 100 s^{-1} (green squares) for the same C = 23.98 % w/w dispersion data shown in Figure S2. The data was collected in the following order: red circles, blue diamonds, and green squares, as indicated by the arrows, with a total measurement time of approximately 8 h.

Relative Zero Shear Viscosity versus Concentration

A plot of the relative zero shear viscosity values $\eta_r = \eta_o/\eta_s$, where η_s is the viscosity of the water solvent, versus concentration C of the aqueous phytoglycogen dispersions is shown in Figure S4. At low values of C, the viscosity of the dispersions remains close to that of water ($\eta_r = 1$). As C is increased, the viscosity increases significantly only after reaching very large values

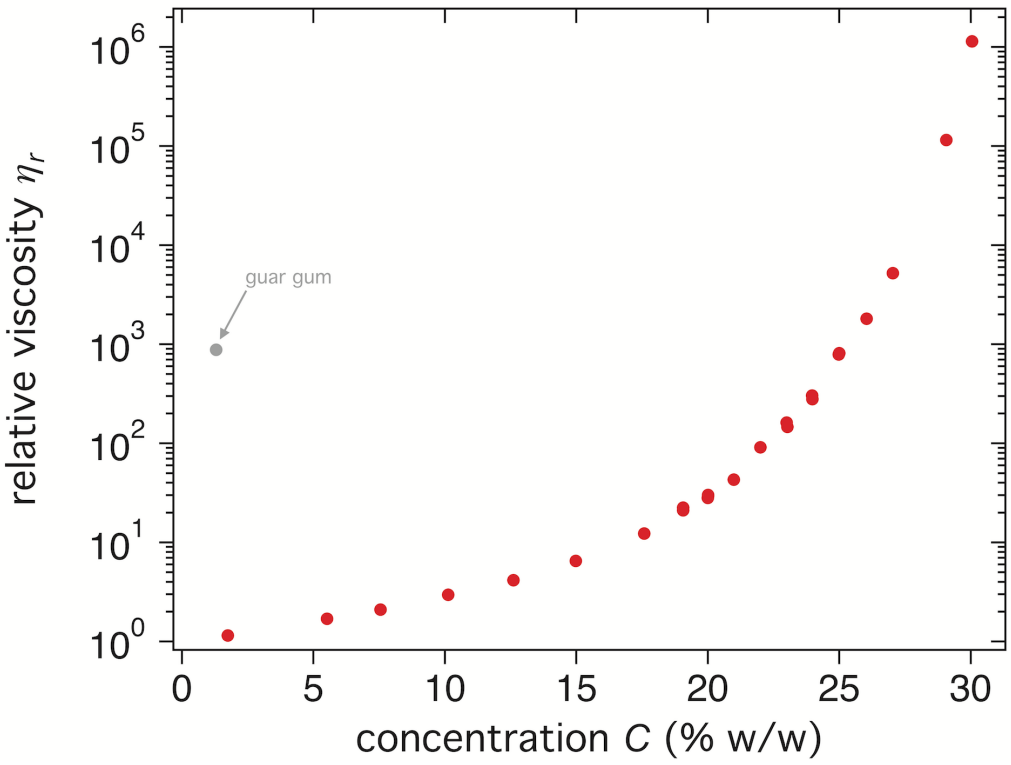

Figure S4: Relative zero shear viscosity η_r as a function of concentration C for aqueous phytoglycogen dispersions (red circles). A data point (grey circle) is also shown for a typical polysaccharide, guar gum, indicating a large value of η_r at a small concentration C = 1.3% w/w.

of the concentration ($C \geq$ 20% w/w). This dependence of η_r on C is very different than that measured for common polysaccharides and gums, for which the viscosity increases significantly for only small amounts of polysaccharides added to water. An example of this is shown as an additional data point (grey circle) in Figure S4, indicating a much larger value of η_r for guar gum at a small value of C = 1.3% w/w.[1] The lack of a significant increase in η_r with increasing C until large values of $C \geq$ 20% w/w are reached (Figure S4) indicates the absence of significant interaction forces between the nanoparticles and is consistent with the exceptional stability of aqueous phytoglycogen dispersions.[2] The dramatic increase of η_r that occurs at very large

concentrations ($C \geq 29\%$ w/w) corresponds to the close packing of the soft, deformable nanoparticles with a correspondingly large value of η_r.

Effective Volume Fraction Calculations

A detailed interpretation of the zero-shear viscosity interactions between the phytoglycogen nanoparticles is enabled by converting the concentration C values to effective volume fraction ϕ_{eff} values. This conversion is complicated by the soft and deformable nature of phytoglycogen as well as their significant uptake of the water solvent. We perform this conversion using two different methods and show that they give consistent results. In the analysis used in the present manuscript, we use the results of Method 2, which is based on an analysis of small angle neutron scattering results.[2]

Method 1

The first method for calculating the effective volume fraction ϕ_{eff} for the dispersions uses the measured η_r values together with the Einstein equation:[3]

$$\eta_r = 1 + 2.5\phi_{\text{eff}}\,, \qquad \text{(S1)}$$

which is valid for colloidal dispersions in the dilute limit. In the dilute limit, the effective volume fraction is proportional to the concentration C, and it can be written as $\phi_{\text{eff}} = kC$. Substituting this expression into Equation S1 gives:

$$\eta_r = 1 + 2.5kC\,. \qquad \text{(S2)}$$

The conversion factor k is determined by fitting the relative zero-shear viscosity η_r versus concentration C data to Equation S2 in the limit of low concentrations. The low concentration ($C \leq 1.5\%$ w/w) η_r versus C data is shown in Figure S5, together with a solid line that was

calculated using the best fit value of k obtained from fitting the red data points to Equation S2. Two symbol colors are shown in Figure S5, corresponding to two different batches of phytoglycogen particles that were extracted, purified and lyophilized using the same procedure. We note the good agreement between the data measured for the two phytoglycogen batches. The best-fit conversion factors were $k = 0.032 \pm 0.003$ for batch 1, and $k = 0.031 \pm 0.003$ for batch 2.

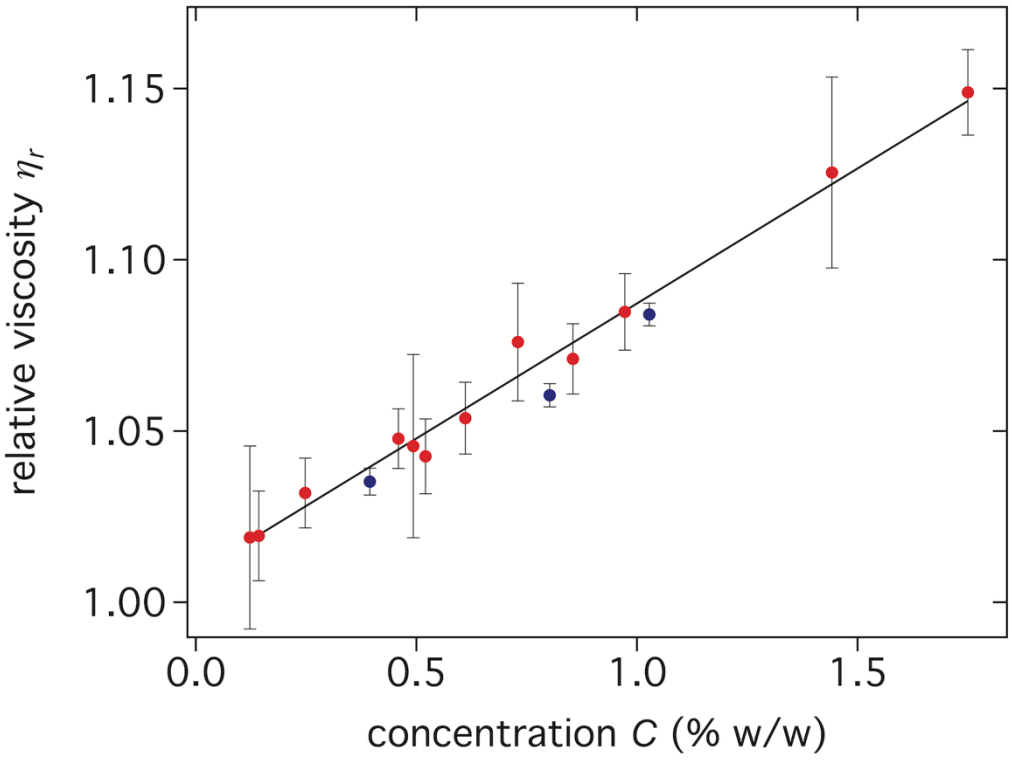

Figure S5: Relative zero-shear viscosity η_r as a function of concentration C for aqueous phytoglycogen dispersions in the dilute limit. These samples were prepared using two different batches of phytoglycogen nanoparticles (represented by red and blue symbols). The solid line is a fit of the red data points to Equation S2: $\eta_r = (1.008 \pm 0.007) + (0.079 \pm 0.008)\, C$, which gives a conversion factor of $k = 0.032 \pm 0.003$. A similar analysis for the blue data points yields a best-fit value of $k = 0.031 \pm 0.003$.

Method 2 (Preferred)

The second and preferred method for calculating the effective volume fraction of phytoglycogen dispersions is based on the measured hydration of the phytoglycogen nanoparticles using small angle neutron scattering (SANS).[2] Contrast matching SANS measurements allowed the determination of the molecular weight of the fully hydrated particles (14.7×10^6 Da) and that of the completely dry particles (4.16×10^6 Da), such that the fully hydrated phytoglycogen nanoparticles contain 253% of their own weight in water.

The w/w ratio of the dispersion is defined as:

$$\mathrm{w/w} = \frac{m_{pgly}}{m_{pgly} + m_{H2O}}, \qquad \text{(S3)}$$

where m_{pgly} is the total mass of the glucose subunits in the dispersion, and m_{H2O} is the total mass of the water in the dispersion, both inside the particles and outside the particles. The concentration C is given by w/w × 100%. If we consider the special case in which we have added just enough particles to eliminate all of the interstitial water, which corresponds to an effective volume fraction $\phi_{\mathrm{eff}} = 1$, the only water in the dispersion is inside the fully hydrated particles. In this case, we can write Eq. S3 as:

$$\frac{\mathrm{w}}{\mathrm{w}} = \frac{m_{pgly}}{\left(m_{pgly} + 2.53 * m_{pgly}\right)} = \frac{1}{3.53} = 0.283 \qquad \text{(S4)}$$

i.e. a concentration of C = 28.3% w/w. Therefore, the effective volume fraction values ϕ_{eff} can be calculated from the concentration C values in % w/w as

$$\phi_{\mathrm{eff}} = kC,$$

where the specific volume conversion factor k = 0.0353. This value of k, which is based on the measured hydration of the phytoglycogen nanoparticles using small angle neutron scattering,

agrees with the value of k = 0.032 ± 0.003 determined by extrapolation from the dilute limit (Method 1) to within experimental uncertainty.

For the analysis performed in the present manuscript, we use the specific volume conversion factor k = 0.0353 determined from the analysis of the SANS data since, compared to Method 1, the uncertainty in the value of k is smaller and it does not rely on a large extrapolation from the dilute limit.

Aging Effects in Phytoglycogen Glasses

In many soft glassy systems, the rheological properties of the material evolve slowly over time, which is referred to as aging.[4,5] Aging effects can be observed in creep relaxation experiments in which a constant shear stress σ is applied to the material and the corresponding time dependence of the shear strain is measured. In Figure S6, we show the results of two successive creep relaxation experiments on a concentrated phytoglycogen sample with ϕ_{eff} = 1.06, in which the shear strain rate $\dot{\gamma}$ is plotted versus time t after a constant shear stress σ is applied. For these experiments, we chose a value of the applied stress that was greater than (100 Pa) and a second value that was less than (5 Pa) the value of the yield stress σ_y = 36 Pa determined from oscillatory amplitude sweep experiments (Figure 4b).

For σ = 100 Pa, the sample had a viscous, liquid-like response and very quickly reached a constant, steady-state plateau in the shear strain rate $\dot{\gamma}$. For σ = 5 Pa, the sample exhibited a fast decay followed by a much slower decay in the shear strain rate $\dot{\gamma}$ that continued for the duration of the experiment (10,000 s). This long-time dependence of $\dot{\gamma}$ for very small stresses is an indication of aging occurring within the sample.

The aging effects presented in Figure S6 are likely only significant in highly concentrated dispersions since dispersions with lower concentrations are much more fluid-like (Figure 4c). We have ensured that aging does not affect our measurements for all concentrations by pre-shearing each sample at a constant shear strain rate of $\dot{\gamma}_{\mathrm{pre-shear}}$ = 100 s^{-1} for 10 min. The shear stresses associated with this value of $\dot{\gamma}_{\mathrm{pre-shear}}$ are well above the yield stress of any of our measured samples, as can be seen from the data presented in Figure 4. For example, for the most concentrated sample, ϕ_{eff} = 1.13, the associated shear stress for an applied shear strain rate of $\dot{\gamma}$ = 100 s^{-1} is 600 Pa, which is much larger than the yield stress value of 160 Pa (Figure 4a). For smaller values of ϕ_{eff}, the ratio of the associated shear stress for $\dot{\gamma}$ = 100 s^{-1} to the yield stress is even larger. Therefore, the pre-shear procedure ensures that our samples are completely fluidized prior to measurement, thus rejuvenating their rheological history and imprinting a known, controllable and reproducible shear history on the sample prior to measurement.[4]

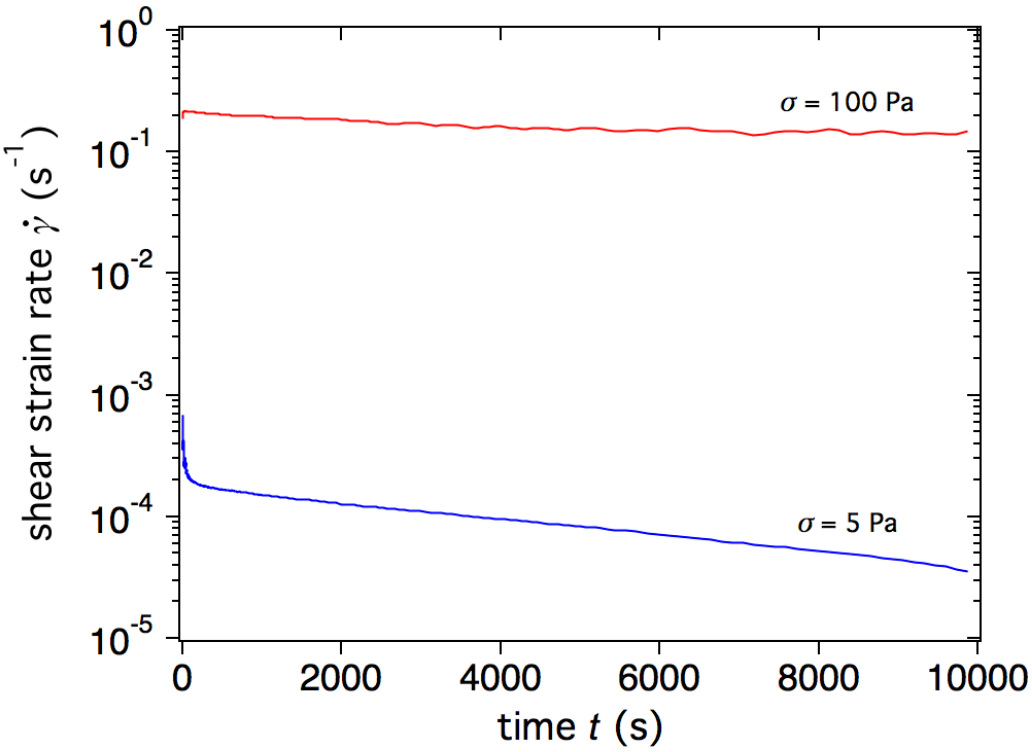

Figure S6: Shear strain rate $\dot{\gamma}$ versus time t for creep relaxation experiments on a phytoglycogen glass with ϕ_{eff} = 1.06. The sample was first subjected to a constant shear stress above its yield stress (red curve; σ = 100 Pa) and then subjected to a constant shear stress below its yield stress (blue curve; σ = 5 Pa).

Dependence of Best-Fit Cross Model Parameters on Concentration

Each of the viscosity η versus shear strain rate $\dot{\gamma}$ data sets shown in Figure 1c shows a power law decrease of η with increasing $\dot{\gamma}$ for sufficiently large values of $\dot{\gamma}$, corresponding to shear thinning. Fitting the data to the modified Cross model (Equation 1) allows the determination of the best-fit values of the zero-shear viscosity η_0, the shear-thinning exponent m and the characteristic time τ. The dependence of the best-fit values of η_0 on dispersion concentration C are shown in Figure S4, the dependence of the best-fit values of m on C are

shown in Figure S7, and the dependence of the best-fit values of τ on C are shown in Figure S8. The best-fit values of m are approximately equal to 0.5 for C < 25% w/w, and they increased approximately linearly with C for larger concentrations (C > 25% w/w) up to a value of 0.78 for C = 32.05% w/w (Figure S7). Because the range of data corresponding to the plateau in the data set for 32.05% w/w at small values of $\dot{\gamma}$ (Figure 1c; data points shown in muted color) is likely due to a wall slip instability, it cannot be included in the fit of the data to Equation 1. Instead, the best-fit m values for C = 32.05% w/w were obtained by fitting the data to a straight line using the same range of high $\dot{\gamma}$ data used to fit Equation 5 to the flow curve data shown in Figure 6.

To a good approximation, the best-fit values of the characteristic time τ increased exponentially with concentration C (Figure S8).

Effect of Wait Time During Steady Shear Measurements

For the steady shear experiments (Figure 1), we tested the effect of increasing the wait or equilibration time between measurements for the sample with C = 30% w/w: by increasing the equilibration time from 5 s to 2000 s, we observed no significant difference between the shear stress values measured at the lowest shear strain rates (Figure S9).

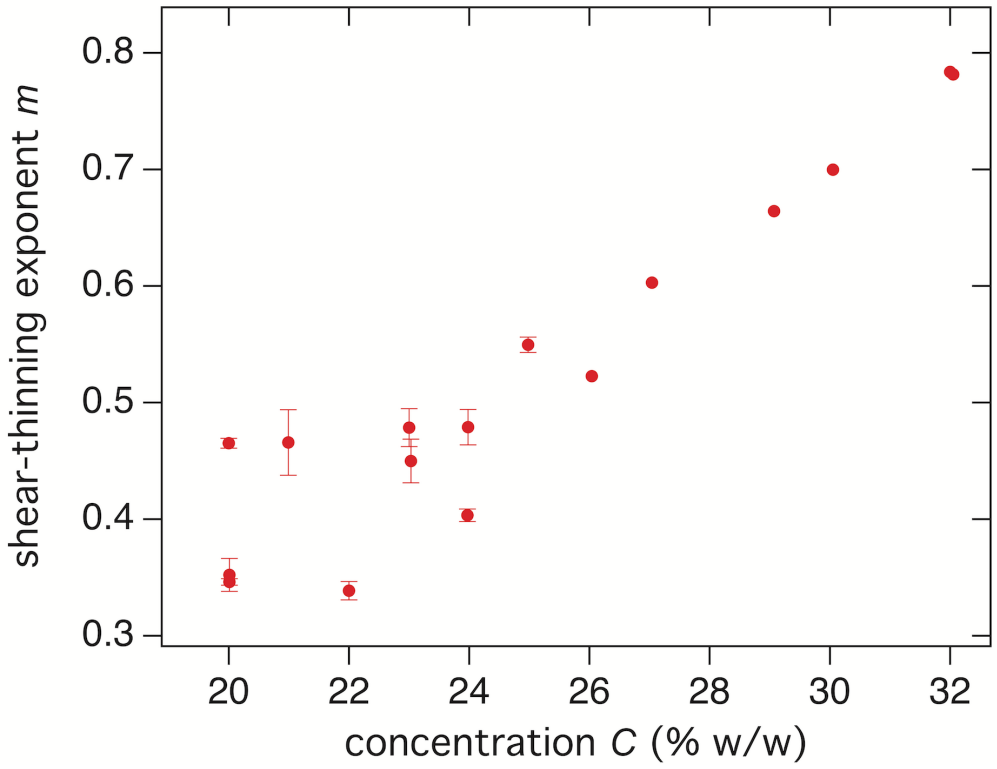

Figure S7: Best-fit values of the shear thinning exponent m obtained by fitting the data shown in Figure 1c to Equation 1, except for the C = 32.05% w/w data points (see text). The error bars correspond to the uncertainties calculated using the least squares fitting procedure.

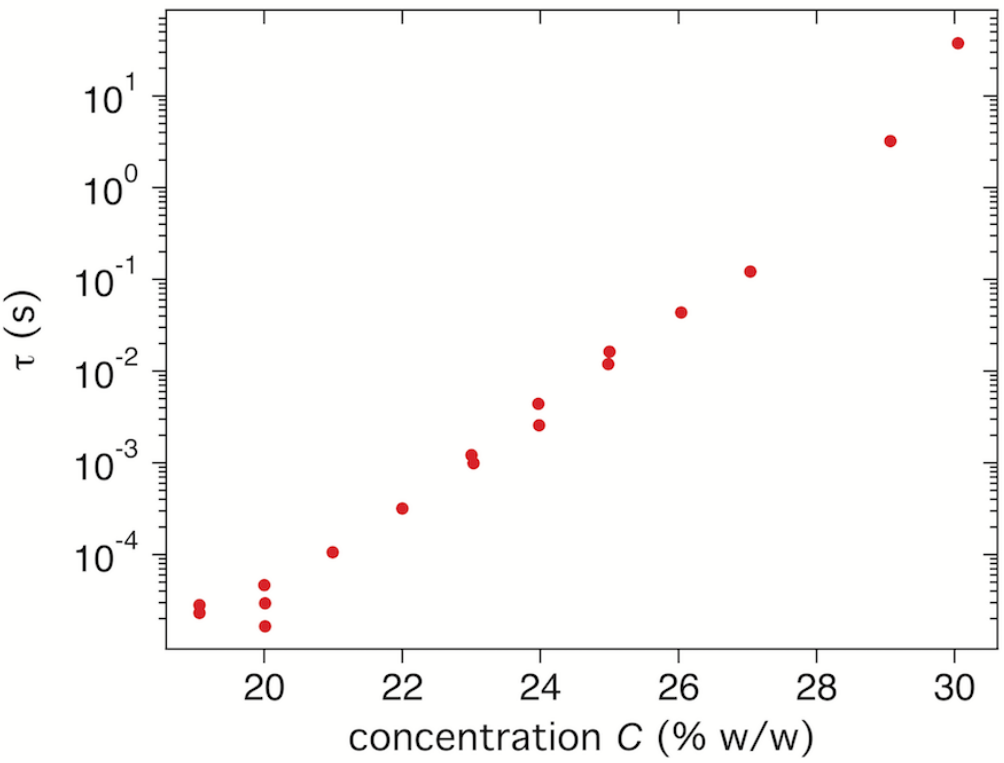

Figure S8: Best-fit values of the characteristic time τ obtained by fitting the data shown in Figure 1c to Equation 1. The error bars corresponding to the uncertainties calculated using the least squares fitting procedure are smaller than the size of the symbols.

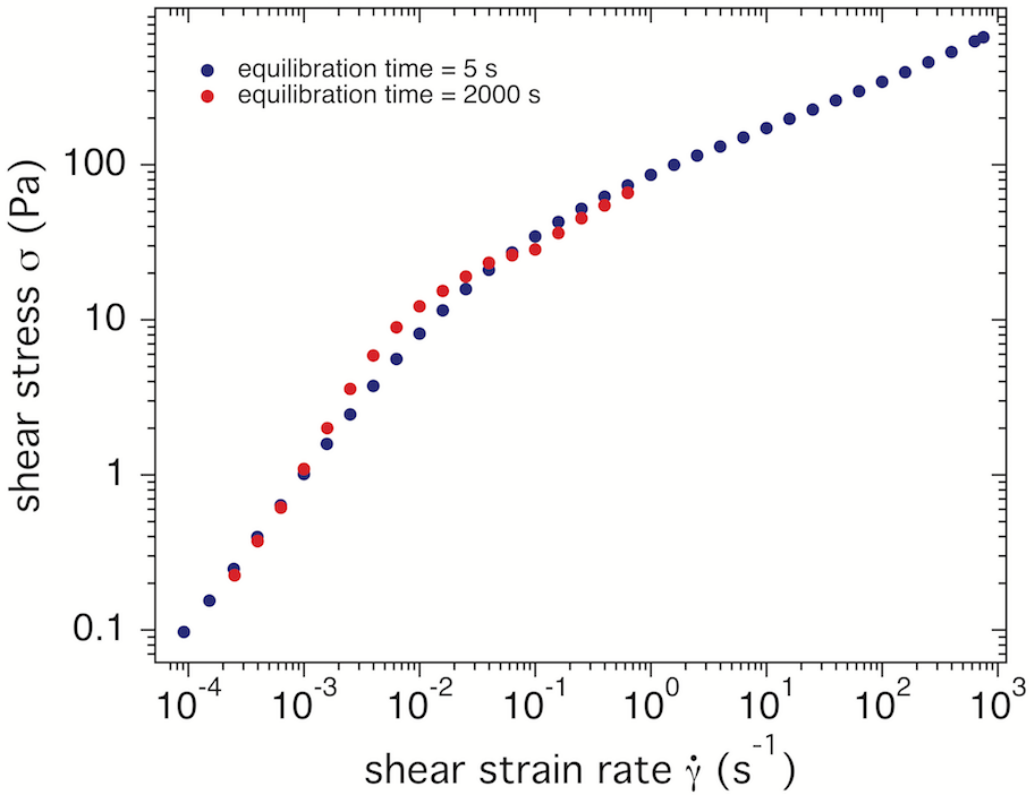

Figure S9: Shear stress σ versus shear strain rate $\dot{\gamma}$ (flow curves) for two different equilibration times between measurements performed for $\dot{\gamma}$ < 1 s-1: 5 s (blue circles; also shown in Figure 1b), and 2000 s (red circles).

References

1 S. P. Patel, R. G. Patel and V. S. Patel, *Int. J. Biol. Macromol.*, 1987, **9**, 314–320.

2 J. D. Nickels, J. Atkinson, E. Papp-Szabo, C. Stanley, S. O. Diallo, S. Perticaroli, B. Baylis, P. Mahon, G. Ehlers, J. Katsaras and J. R. Dutcher, *Biomacromolecules*, 2016, **17**, 735–743.

3 A. Einstein, *Ann. Phys.*, 1906, **324**, 289–306.

4 B. M. Erwin, M. Cloitre, M. Gauthier and D. Vlassopoulos, *Soft Matter*, 2010, **6**, 2825–2833.

5 B. M. Erwin, D. Vlassopoulos, M. Gauthier and M. Cloitre, *Phys. Rev. E*, 2011, **83**, 061402.